ARTICLES

Direct conversion of fibroblasts to functional neurons by defined factors

Thomas Vierbuchen[1,2], Austin Ostermeier[1,2], Zhiping P. Pang[3], Yuko Kokubu[1], Thomas C. Südhof[3,4] & Marius Wernig[1,2]

Cellular differentiation and lineage commitment are considered to be robust and irreversible processes during development. Recent work has shown that mouse and human fibroblasts can be reprogrammed to a pluripotent state with a combination of four transcription factors. This raised the question of whether transcription factors could directly induce other defined somatic cell fates, and not only an undifferentiated state. We hypothesized that combinatorial expression of neural-lineage-specific transcription factors could directly convert fibroblasts into neurons. Starting from a pool of nineteen candidate genes, we identified a combination of only three factors, *Ascl1*, *Brn2* (also called *Pou3f2*) and *Myt1l*, that suffice to rapidly and efficiently convert mouse embryonic and postnatal fibroblasts into functional neurons *in vitro*. These induced neuronal (iN) cells express multiple neuron-specific proteins, generate action potentials and form functional synapses. Generation of iN cells from non-neural lineages could have important implications for studies of neural development, neurological disease modelling and regenerative medicine.

The diverse cell types present in the adult organism are produced during development by lineage-specific transcription factors that define and reinforce cell-type-specific gene expression patterns. Cellular phenotypes are further stabilized by epigenetic modifications that allow faithful transmission of cell-type-specific gene expression patterns over the lifetime of an organism[1,2]. Recent work showing that four transcription factors are sufficient to induce pluripotency in primary fibroblasts demonstrated that fully differentiated cells can be induced to undergo dramatic cell fate changes[3]. Similarly, the transfer of somatic cell nuclei into oocytes, as well as cell fusion of pluripotent cells with differentiated cells, have proven to be capable of inducing pluripotency[4–9]. This remarkable transformation has been interpreted as a reversion of mature into more primitive developmental states, with a concomitant erasure of developmentally relevant epigenetic information[10]. Therefore, direct reprogramming between divergent lineages could be unique to reprogramming into an embryonic state, and might not be possible between different somatic cell states. However, cell fusion or forced expression of lineage-specific genes in somatic cells can induce traits of other cell types[11,12]. For example, the basic helix–loop–helix (bHLH) transcription factor *MyoD* (also called *Myod1*) can induce muscle-specific properties in fibroblasts but not hepatocytes[13,14]; ectopic expression of interleukin (IL)-2 and granulocyte–macrophage colony-stimulating factor receptors can lead to myeloid conversion in committed lymphoid progenitor cells[15]; expression of *Cebpa* in B cells or *PU.1* (also called *Sfpi1*) and *Cebpa* in fibroblasts induces characteristics of macrophages[16–18]; deletion of *Pax5* can induce B cells to de-differentiate towards a common lymphoid progenitor[19]; and the bHLH transcription factor neurogenin 3, in combination with *Pdx1* and *Mafa*, can efficiently convert pancreatic exocrine cells into functional β-cells *in vivo*[20]. Here, we set out to determine whether specific transcription factors could directly convert fibroblasts into functional neurons.

A screen for neuronal-fate-inducing factors

Reasoning that multiple transcription factors would probably be required to reprogram fibroblasts to a neuronal fate, we cloned a total of 19 genes that are specifically expressed in neural tissues, have important roles in neural development, or have been implicated in epigenetic reprogramming (Supplementary Table 1). A pool of lentiviruses containing all 19 genes (19F pool) was prepared to infect mouse embryonic fibroblasts (MEFs) from TauEGFP knock-in mice, which express EGFP specifically in neurons[21,22] (see Fig. 1a for experimental outline). Great care was taken to exclude neural tissue from the MEF preparation, and we were unable to detect evidence for the presence of neurons or neural progenitor cells in these cultures using immunofluorescence, fluorescence activated cell sorting (FACS) and polymerase chain reaction with reverse transcription (RT–PCR) analyses (Supplementary Fig. 1). However, uninfected MEFs did contain rare Tuj1-positive, TauEGFP-negative cells with fibroblast-like morphology, indicative of weak Tuj1 (that is, β-III-tubulin) expression in non-neuronal cells (Fig. 1b, c and Supplementary Fig. 1a). In contrast, 32 days after infection with the 19F pool, we detected Tuj1-positive cells with typical neuronal morphologies and bright TauEGFP fluorescence (Fig. 1d,e). Thus, some combination(s) of the genes in the 19F pool was capable of converting MEFs into iN cells.

We next set out to narrow down the number of transcription factors required for generation of iN cells. Given their important roles in neuronal cell fate determination[23–26] we first tested the bHLH transcription factors *Ascl1* (also known as *Mash1*) and *Neurod1* individually. Notably, we observed occasional Tuj1-positive, TauEGFP-positive cells exhibiting a simple mono- or bipolar morphology after infection with only *Ascl1* (Supplementary Fig. 2b). However, 19F iN cells showed more complex morphologies, which indicated that the activity of *Ascl1* alone was not sufficient to recapitulate the full activity of the 19F pool (compare to Fig. 1d, e). We therefore tested the neuron-inducing activity of *Ascl1* in combination with each of the remaining 18 candidate genes (Supplementary Fig. 2a). Five genes (*Brn2*, *Brn4* (*Pou3f4*), *Myt1l*, *Zic1* and *Olig2*) substantially potentiated the neuron-inducing activity of *Ascl1* (Supplementary Fig. 2a, b). Importantly, none of these five genes generated iN cells when tested individually (data not shown). Next, we tested whether combinatorial expression of these factors with *Ascl1* could further increase the induction of neuron-like cells by infecting

[1]Institute for Stem Cell Biology and Regenerative Medicine, Department of Pathology, [2]Program in Cancer Biology, [3]Department of Molecular and Cellular Physiology, [4]Howard Hughes Medical Institute, Stanford University School of Medicine, 1050 Arastradero Road, Palo Alto, California 94304, USA.

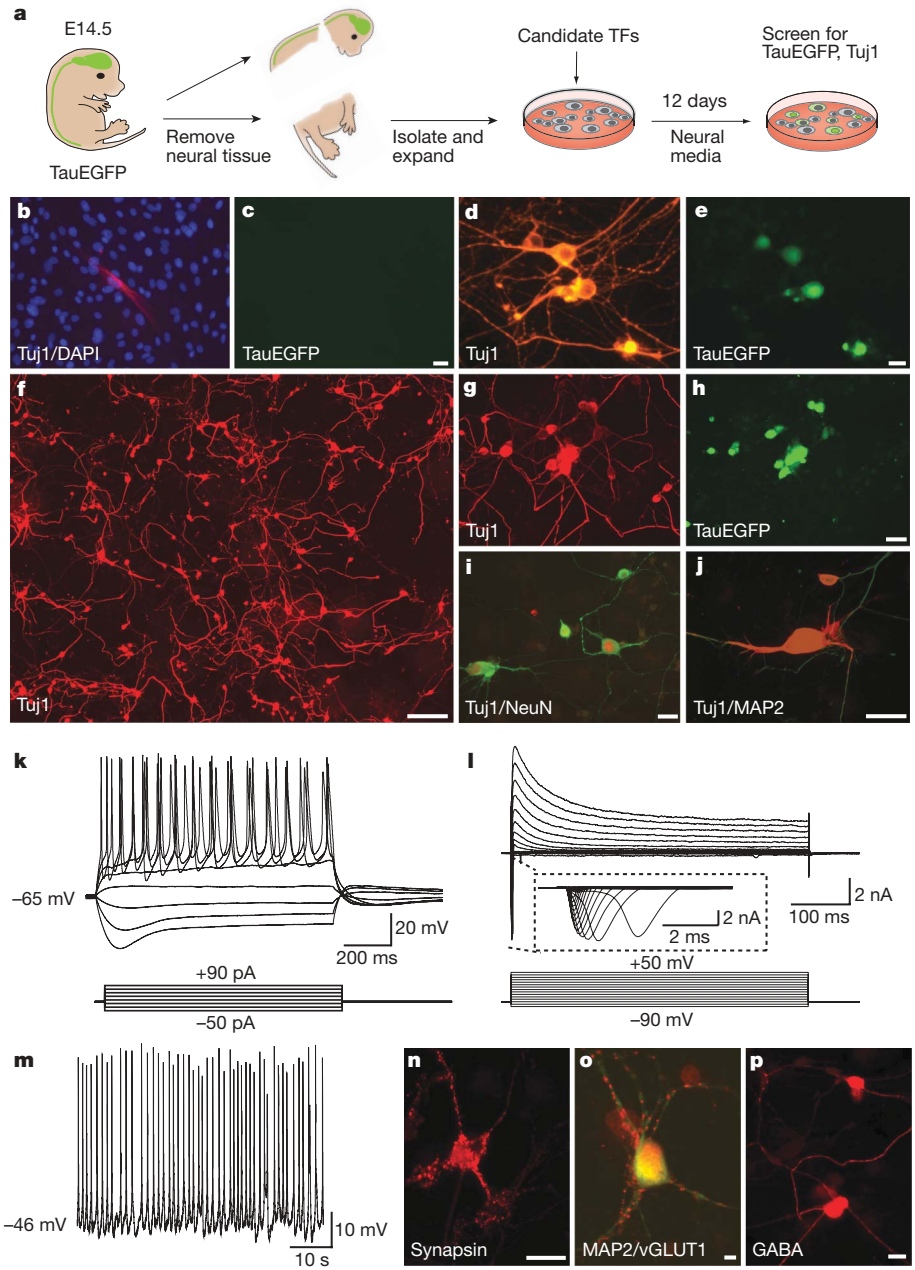

Figure 1 | A screen for neuronal-fate-inducing factors and characterization of MEF-derived iN cells **a**, Experimental rationale. **b**, Uninfected, p3 TauEGFP MEFs contained rare Tuj1-positive cells (red) with flat morphology. Blue indicates 4,6-diamidino-2-phenylindole (DAPI) counterstain. **c**, Tuj1-positive fibroblasts do not express visible TauEGFP. **d**, **e**, MEF iN cells express Tuj1 (red) and TauEGFP (green) and display complex neuronal morphologies 32 days after infection with the 19-factor (19F) pool. **f**, Tuj1 expression in MEFs 13 days after infection with the 5F pool. **g**–**j**, MEF-derived Tuj1-positive iN cells co-express the pan-neuronal markers TauEGFP (**h**), NeuN (red, **i**) and MAP2 (red, **j**). **k**, Representative traces of membrane potential responding to step depolarization by current injection (lower panel). Membrane potential was current-clamped at around −65 mV. **l**, Representative traces of whole-cell currents in voltage-clamp mode; cells were held at −70 mV; step depolarization from −90 mV to +50 mV at 10-mV intervals was delivered (lower panel). The inset shows Na^+ currents. **m**, Spontaneous action potentials recorded from a 5F MEF iN cell 8 days after infection. No current injection was applied. **n**–**p**, Twenty-two days after infection 5F MEF iN cells expressed synapsin (red, **n**) and vesicular glutamate transporter 1 (vGLUT1; red, **o**) or GABA (**p**). Scale bars: 5 μm (**o**), 10 μm (**e**, **j**, **n**, **p**) 20 μm (**c**, **h**, **i**) and 200 μm (**f**).

TauEGFP MEFs with a pool of *Brn2*, *Myt1l*, *Zic1*, *Olig2* and *Ascl1* viruses (5F pool). Given its close similarity to *Brn2*, we did not include *Brn4* in the 5F pool. Twelve days after infection, we detected frequent Tuj1-positive iN cells with highly complex morphologies (Fig. 1f). These 5F iN cells also expressed the pan-neuronal markers MAP2, NeuN and synapsin (Fig. 1i–j, n). Similar results were obtained with iN cells derived from BALB/c MEFs (Supplementary Fig. 3a).

Characterization of 5-factor iN cells

To explore whether iN cells have functional membrane properties similar to neurons, we performed patch-clamp recordings of TauEGFP-positive cells on days 8, 12 and 20 after infection. For the majority of the iN cells analysed (85.1%, $n = 47$), action potentials could be elicited by depolarizing the membrane in current-clamp mode (Fig. 1k). Six cells (14.2%, $n = 42$) showed spontaneous action potentials, some as early as 8 days after transduction (Fig. 1m). These action potentials could be blocked by tetrodotoxin (TTX), a specific inhibitor of Na^+ ion channels (Supplementary Fig. 3e). Moreover, in voltage-clamp mode we observed both fast, inactivating inward and outward currents, which probably correspond to opening of voltage-dependent K^+- and Na^+-channels, respectively, with a possible contribution of Ca^{2+} channels to the whole-cell currents (Fig. 1l and

Supplementary Fig. 3f). The resting membrane potentials ranged between −30 and −69 mV with an average of ∼−55 mV on day 20 ($n = 12$, Supplementary Tables 2 and 3). Additionally, we asked whether these cells possessed functional ligand-gated ion channels. Induced neuronal cells responded to exogenous application of GABA (γ-aminobutyric acid), and this response could be blocked by the GABA receptor antagonist picrotoxin (Supplementary Fig. 3g). Thus, MEF-derived iN cells seem to exhibit the functional membrane properties of neurons and possess ligand-gated GABA receptors.

We then sought to characterize the neurotransmitter phenotype of iN cells. After 21 days of culture in minimal neuronal media, we detected vGLUT1-positive puncta outlining MAP2-positive neurites of some cells, indicating the presence of excitatory, glutamatergic neurons (Fig. 1o). In addition, we found iN cells labelled with antibodies against GABA, the major inhibitory neurotransmitter in brain (Fig. 1p). Some iN cells (9 out of ∼500) contained the Ca^{2+}-binding protein calretinin, a marker for cortical interneurons and other neuronal subtypes (Supplementary Fig. 3c). No expression of tyrosine hydroxylase, choline acetyltransferase or serotonin was detected. The vast majority of iN cells were negative for peripherin, an intermediate filament characteristic of peripheral neurons (data not shown)[27].

Functional neurons from tail fibroblasts

To evaluate whether iN cells could also be derived from postnatal cells, we isolated tail-tip fibroblasts (TTFs) from 3-day-old TauEGFP and Rosa26-rtTA mice[28]. Similar to our MEF cultures, we could not detect pre-existing neurons, glia, or neural progenitor cells (Supplementary Fig. 1a). Twelve days after infecting TTFs with the 5F pool, Tuj1-positive iN cells with a complex, neuronal morphology could be readily detected (Fig. 2a). TTF iN cells expressed the pan-neuronal markers NeuN, MAP2 and synapsin (Fig. 2b, c, f). Electrophysiological recordings 12 days after infection demonstrated an average resting membrane potential of ∼−57 mV (range: −35 to −70 mV, $n = 11$), firing of action potentials (81.8%, $n = 11$) (Fig. 2d),

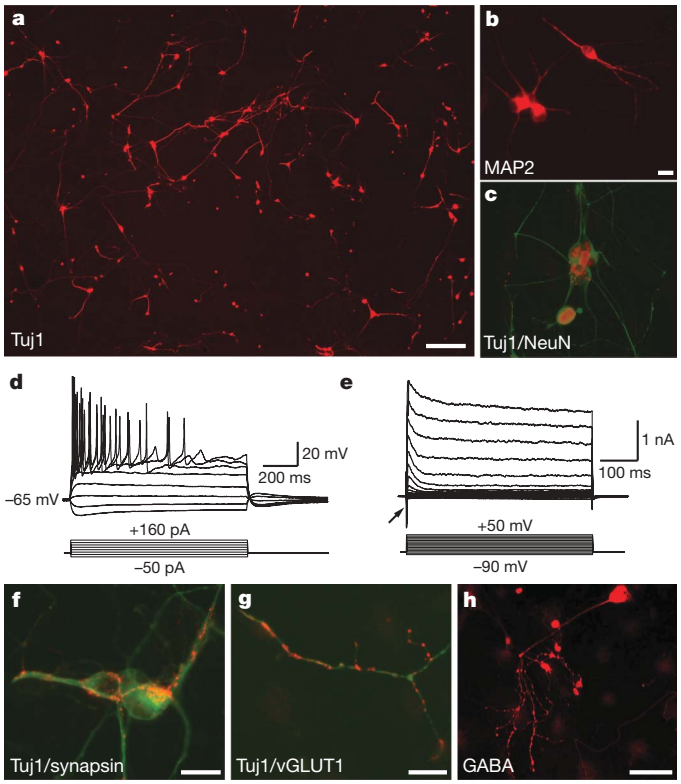

Figure 2 | Efficient induction of neurons from perinatal tail-tip fibroblasts **a**, Tuj1-stained tail-tip fibroblast (TTF) 13 days after infection with the 5F pool. **b**, **c**, TTF iN cells express the pan-neuronal markers MAP2 (**b**) and NeuN (**c**). **d**, Representative traces showing action potentials elicited at day 13 after infection. Nine of eleven cells recorded exhibited action potentials. **e**, Whole-cell currents recorded in voltage-clamp mode. Inward fast inactivating Na^+ currents (arrow) and outward currents can be observed. **f–h**, At 21 days after infection TTF iN cells express synapsin (red, **f**), vGLUT1 (red, **g**) and GABA (**h**). **c**, **f** and **g** are overlay images with the indicated marker (red) and Tuj1 (green). Scale bars: 20 μm (**b**, **f**, **g**), 100 μm (**h**), 200 μm (**a**).

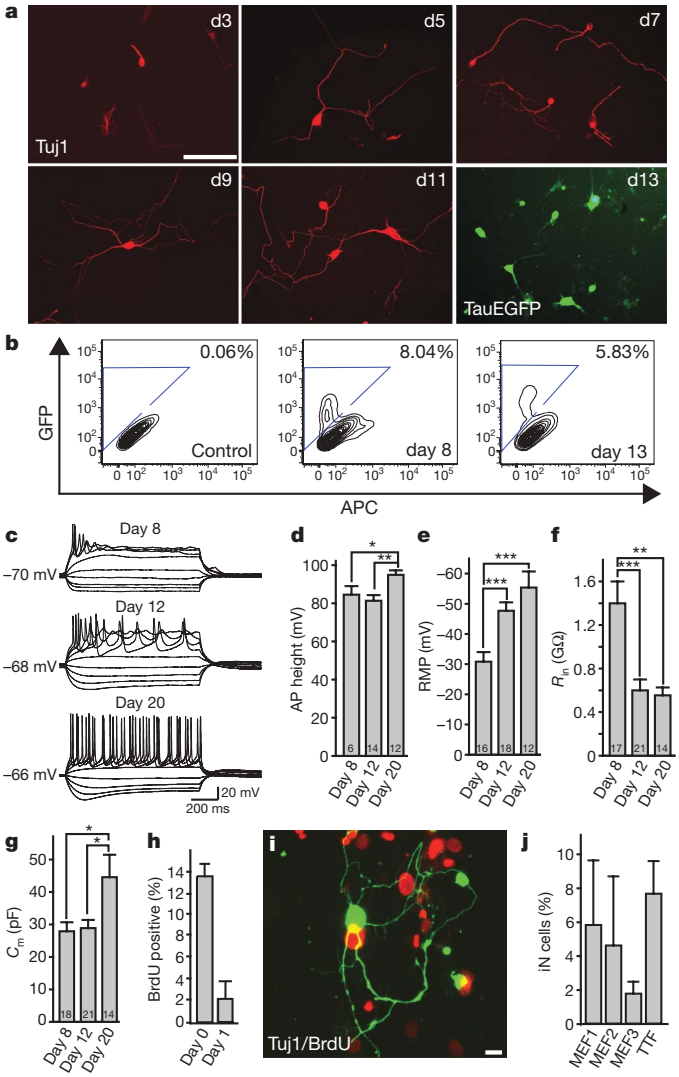

Figure 3 | The 5F-pool-induced conversion is rapid and efficient **a**, Tuj1-positive iN cells (red) show morphological maturation over time after viral infections. At day 13, TauEGFP expression outlines neuronal processes. **b**, FACS analysis of TauEGFP expression 8 and 13 days after infection. Control indicates uninfected TauEGFP MEFs. APC, allophycocyanin. **c**, Representative traces showing action potentials elicited from MEF iN cells at days 8, 12 and 20 after infection. Cells were maintained at a potential of approximately −65 to −70 mV. Step current injection protocols were used from −50 to +70 pA. Scale bar applies to all traces. **d–g**, Quantification of membrane properties in MEF iN cells at 8, 12 and 20 days after infection. Numbers in the bars represent the numbers of recorded cells. Data are presented as mean ± s.e.m. $*P < 0.05$; $**P < 0.01$; $***P < 0.001$ (Student's t-test). AP, action potential; C_m, membrane capacitance; R_{in}, membrane input resistances; RMP, resting membrane potential. Action potential heights were measured from the baseline. **h**, BrdU-positive iN cells after BrdU treatment from day 0–13 or day 1–13 after transgene induction. **i**, Example of a Tuj1 (green) positive cell not labelled with BrdU (red) when added at day 0 after addition of doxycycline. Data are presented as mean ± s.d. **j**, Efficiency estimates for iN cell generation 13 days after infection (see Methods). Every bar represents an independent experiment. Doxycycline was added 48 h after plating in MEF experiment 1 and after 24 h in MEF experiments 2 and 3. Error bars indicate ± s.d. of cell counts. Scale bars: 10 μm (**i**), 100 μm (**a**).

and expression of functional voltage-gated membrane channel proteins (Fig. 2e and Supplementary Tables 2 and 3). We were also able to detect vGLUT1-positive as well as GABA-positive cells (Fig. 2g, h). Despite extensive screening (>1,000 iN cells analysed), we were unable to detect tyrosine hydroxylase, choline acetyltransferase, or serotonin expression. Induced neuronal cells exhibited rare peripherin-positive filaments (Supplementary Fig. 3d).

Neuronal induction is fast and efficient

Next, we assessed the kinetics and efficiency of 5F iN conversion. In MEFs, Tuj1-positive cells with immature neuron-like morphology were found as early as 3 days after infection (Fig. 3a). After 5 days, neuronal cells with long, branching processes were readily detected, and over time increasingly complex morphologies were evident, suggesting an active process of maturation in newly formed iN cells (Fig. 3a). Similarly, we detected TauEGFP expression as early as day five (Supplementary Fig. 3h). The fraction of TauEGFP-positive cells remained similar at 8 and 13 days after infection, as determined by FACS analysis, indicating no *de novo* generation of iN cells after day 8 (Fig. 3b). Electrophysiological parameters such as action potential height, resting membrane potential, membrane input resistance and membrane capacitance also showed signs of maturation over time (Fig. 3c–g and Supplementary Tables 2 and 3).

To estimate the conversion efficiency, we first determined how many of the MEF-derived iN cells divided after induction of the viral transgenes by treating the cells with 5-bromodeoxyuridine (BrdU) throughout the duration of the culture period and beginning 1 day after gene induction. The results showed that the vast majority of iN cells became post mitotic by 24 h after transgene activation (Fig. 3h, i). This allowed us to roughly estimate the conversion efficiency of our method by quantifying the total number of Tuj1-positive iN cells in the entire dish on day 12, and dividing this number by the number of plated cells (see Methods). Using this method, the efficiency ranged from 1.8% to 7.7% in MEF and TTF iN cells (Fig. 3j) presumably due to slight variations in titres of the viruses. These calculations might be an underestimation of the true conversion rate because not all cells receive the necessary complement of viral transgenes.

iN cells form functional synapses

Because iN cells exhibited the membrane properties of neurons, we next wanted to assess whether iN cells have the capacity to form functional synapses. To accomplish this we used two independent methods. First, we determined whether iN cells were capable of synaptically integrating into pre-existing neural networks. We used FACS to purify TauEGFP-positive iN cells 7 days after infection and re-plated the 5F iN cells onto neonatal cortical neurons that had been cultured for 7 days *in vitro*. One week after re-plating, we performed patch-clamp recordings from TauEGFP-positive iN cells and observed spontaneous and rhythmic network activity typical of cortical neurons in culture (Fig. 4a, b). Both excitatory and inhibitory postsynaptic currents (EPSCs and IPSCs) could be evoked after electrical stimulation delivered from a concentric electrode placed 100–150 μm away from the patched iN cells (Fig. 4b–d). In the presence of the α-amino-3-hydroxy-5-methyl-4-isoxazole propionic acid (AMPA) and NMDA (*N*-methyl-D-aspartate) receptor channel blockers 6-cyano-7-nitroquinoxaline-2,3-dione (CNQX) and D(-)-2-amino-5-phosphonovaleric acid (D-AP5), spontaneous IPSCs were reliably detected (Fig. 4c, upper panel). Evoked IPSCs could be blocked by further addition of picrotoxin (Fig. 4c, middle panel). Similarly, at a holding potential of −70 mV and in the presence of picrotoxin, fast-decaying EPSCs mediated by AMPA receptors could be evoked (Fig. 4d, middle panel). Conversely, at a holding potential of +60 mV (which relieves the voltage-dependent blockade of

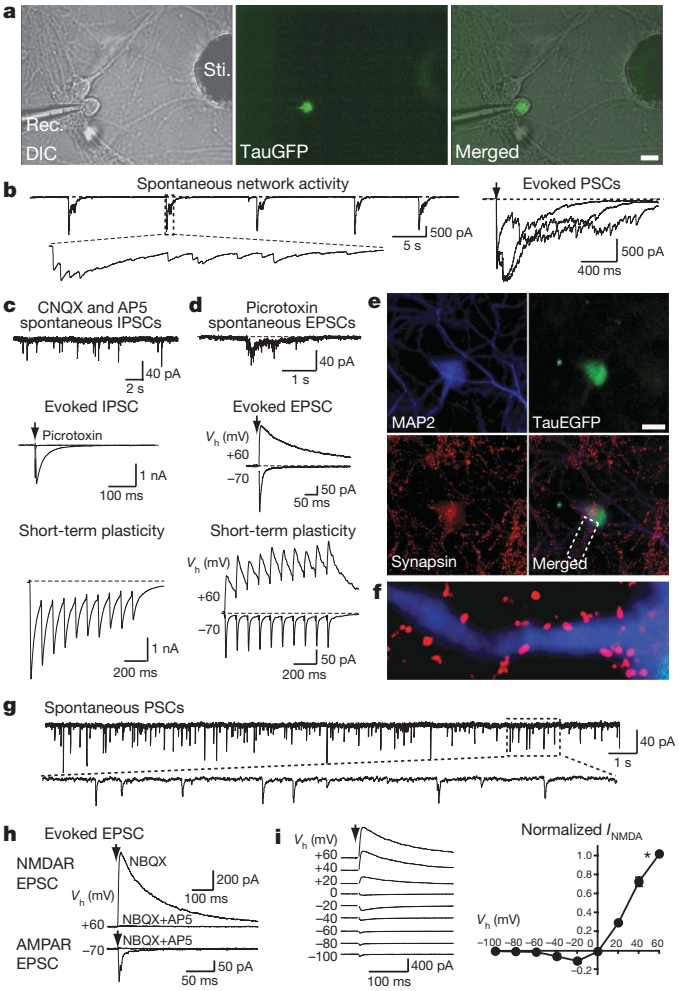

Figure 4 | MEF-derived iN cells show functional synaptic properties. TauEGFP-positive iN cells were FACS purified 7–8 days after infection of MEFs and plated on cortical neuronal cultures (7 days *in vitro*, **a**–**f**) or on monolayer glia cultures (**g**–**i**). Electrophysiological recordings were performed 7–20 days after sorting. **a**, Recording electrode (Rec.) patched onto an TauEGFP-positive cell (middle panel) with a stimulation electrode (Sti.). The right panel is a merged picture of DIC and fluorescence images showing that the recorded cell is TauEGFP positive. **b**, Representative traces of spontaneous synaptic network activities and representative evoked postsynaptic currents (PSCs) after stimulation. **c**, In the presence of 20 μM CNQX and 50 μM D-AP5, a representative trace of spontaneous IPSCs is shown (upper panel). Evoked IPSCs could be elicited (middle panel) and blocked by the addition of picrotoxin. When a train of 10 stimulations was applied at 10 Hz, evoked IPSCs show depression (lower panel). **d**, In the presence of 30 μM picrotoxin, excitatory synaptic activities from EGFP-positive cells were observed. Spontaneous (upper panel) and evoked (middle panel) EPSCs are shown. At a holding potential (V_h) of −70 mV, AMPA receptor (AMPAR)-mediated EPSCs were monitored. When the holding potentials were set at +60 mV, both AMPAR- and NMDAR-mediated EPSCs could be recorded. The lower panel shows the short-term synaptic plasticity of both AMPAR- and NMDAR-mediated synaptic activities. Arrows indicate time of stimulation. **e**, Example of a TauEGFP-positive iN cell expressing MAP2 among cortical neurons. **f**, Higher magnification (×7) of area marked in **e**. **g**, Representative spontaneous postsynaptic currents (PSCs) recorded from MEF iN cells co-cultured with glia. **h**, Representative traces of evoked EPSCs. NMDAR-mediated EPSCs in the presence of 10 μM NBQX (2,3-dihydroxy-6-nitro-7-sulphamoyl-benzo[f]quinoxaline-2,3-dione), an AMPA-receptor antagonist, were recorded at a holding potential (V_h) of +60 mV. Application of D-AP5 blocked the response. AMPAR-mediated EPSCs were recorded at a V_h of −70 mV. The AMPAR-evoked response is blocked by NBQX and AP5. **i**, Current–voltage (*I*–*V*) relationship of NMDAR-mediated EPSCs (left panel); representative traces of evoked EPSCs at different V_h as indicated. The right panel shows the summarized *I*–*V* relationship. NMDAR EPSC amplitudes (I_{NMDA}) are normalized to EPSCs at a V_h of +60 mV (indicated by an asterisk, $n = 5$). NMDAR EPSCs show ratifications at negative holding potentials, presumably because of the blockade of NMDAR by Mg^{2+}. Scale bars: 10 μm (**a**, **e**).

Mg^{2+} to NMDA receptors), slow-decaying NMDA-receptor-mediated EPSCs could be recorded (Fig. 4d, middle panel).

Moreover, synaptic responses recorded from iN cells showed signs of short-term synaptic plasticity, such as depression of IPSCs and facilitation of EPSCs during a high-frequency stimulus train (Fig. 4c, d, lower panels). The presence of synaptic contacts between iN cells and cortical neurons was independently corroborated by the immunocytochemical detection of synapsin-positive puncta surrounding MAP2-positive dendrites originating from EGFP-positive cells (Fig. 4e, f). We were also able to observe synaptic responses in similar experiments performed with iN cells derived from TTFs (Supplementary Fig. 4). These data demonstrate that iN cells can form functional postsynaptic compartments and receive synaptic inputs from cortical neurons.

Next we asked whether iN cells were capable of forming synapses with each other. To address this question we plated FACS-sorted TauEGFP-positive, MEF-derived 5F iN cells 8 days after infection onto a monolayer culture of primary astrocytes, which are thought to have an essential role in synaptogenesis[29,30]. Importantly, we confirmed that these cultures were free of pre-existing Tuj1- or MAP2-positive neurons (data not shown). Patch-clamp recordings at 12–17 days after sorting indicated the presence of spontaneous postsynaptic currents in 5 out of 11 cells (Fig. 4g). Upon extracellular stimulation, evoked EPSCs could be elicited in a majority of the cells (9 out of 11 cells, Fig. 4h). Similar to iN cells cultured with primary cortical neurons, we were able to record both NMDA-receptor-mediated (9 out of 11 cells) and AMPA-receptor-mediated EPSCs (8 out of 11 cells; Fig. 4h, i). Interestingly, we were unable to detect obvious IPSCs in a total of 15 recorded 5F iN cells. These data indicate that iN cells are capable of forming functional synapses with each other, and that the majority of iN cells exhibit an excitatory phenotype.

Genes sufficient for neuronal conversion

As stated earlier, *Ascl1* was the only gene from the 5F pool that was sufficient to induce neuron-like cells in MEFs. We next attempted to determine the relative contribution of each of the five genes by removing each gene from the pool and assessing the efficiency of iN cell generation. Surprisingly, only the omission of *Ascl1* had a marked effect on induction efficiency (Supplementary Fig. 6a). Thus, we tested the effects of removing two genes at a time by evaluating all possible three-gene combinations. Our results indicated that either *Ascl1* or both *Brn2* and *Myt1l* must be present to generate iN cells (Fig. 5a). The most efficient conversions were achieved when *Ascl1* and *Brn2* were combined with either *Myt1l* (BAM pool) or *Zic1* (BAZ pool). The efficiencies in these conditions were two- to three-fold higher than the 5F pool when the total amount of virus was kept constant (Fig. 5a–d). In this experiment the BAM iN cells appeared to have a more complex morphology than the BAZ cells (Fig. 5c, d and Supplementary Fig. 7). Therefore, we focused our further analysis on the BAM pool.

MEF-derived BAM iN cells expressed the pan-neuronal markers MAP2 and synapsin (Fig. 5f). The BAM pool was capable of efficiently generating iN cells from perinatal TTFs (Fig. 5e and Supplementary Fig. 8a–e). After infecting TTFs from adult mice with these three factors, we could detect neuronal cells expressing TauEGFP, Tuj1, NeuN and MAP2 (Supplementary Fig. 9). Importantly, when co-cultured with astrocytes, both MEF and perinatal TTF-derived BAM iN cells were capable of forming functional synapses as determined by the presence of both NMDA- and AMPA-receptor mediated EPSCs (Fig. 5g, h). Similar to 5F iN cells, no IPSCs were detected in MEF-derived ($n = 16$) or TTF-derived ($n = 12$) BAM iN cells. This functional evidence indicates that a majority of BAM iN cells are excitatory. Indeed, 53% (111 out of 211 cells) of MEF BAM iN cells expressed Tbr1, a marker of excitatory cortical neurons, whereas less than 1% (3 out of ~500 cells) were GAD-positive (Supplementary Fig. 8f).

Our results left open the possibility that one or two factors might be able to induce functional neuronal properties in MEFs. Thus, we tested

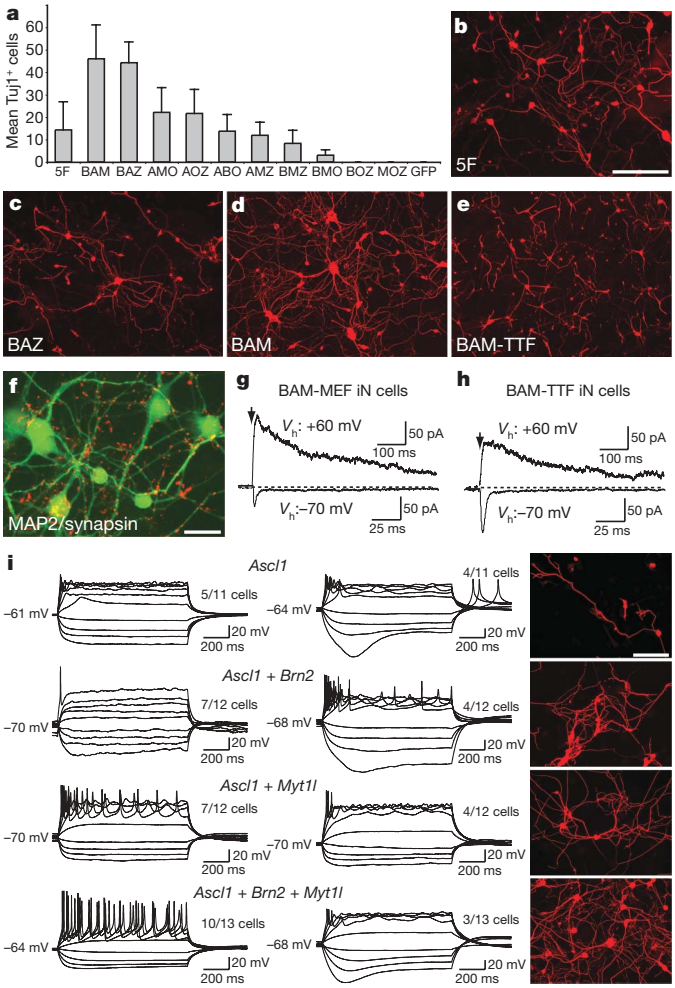

Figure 5 | Defining a minimal pool for efficient induction of functional iN cells a, Quantification of Tuj1-positive iN cells from TauEGFP MEFs infected with different three-factor combinations of the five genes. Each gene is represented by the first letter in its name. A, *Ascl1*; B, *Brn2*; M, *Myt1l*; O, *Olig2*; Z, *Zic1*. Averages from 30 randomly selected visual fields are shown (error bars indicate ±s.d.). **b–d**, Representative images of Tuj1 staining of MEFs infected with the 5F (**b**), *Ascl1* + *Brn2* + *Zic1* (BAZ; **c**) and *Ascl1* + *Brn2* + *Myt1l* (BAM; **d**) pools. **e**, Tuj1 staining of perinatal TTF iN cells 13 days after infection with the BAM pool. **f**, BAM-induced MEF iN cells express MAP2 (green) and synapsin (red) 22 days after infection. **g**, Representative traces of synaptic responses recorded from MEF-derived BAM (3F) iN cells co-cultured with glia after isolation by FACS. V_h, holding potential. At a V_h of −70 mV, AMPAR-mediated EPSCs were recorded; at a V_h of +60 mV, NMDAR-mediated EPSCs were revealed. **h**, Synaptic responses recorded from TTF-derived 3F iN cells. **i**, Representative traces of action potentials elicited from MEF-derived iN cells transduced with the indicated gene combinations, recorded 12 days after infection. Cells were maintained at a resting membrane potential of approximately −65 to −70 mV. Step current injection protocols were used from −50 to +70 pA. Traces in each subgroup (left or right panels) represent subpopulations of neurons with similar responses. Numbers indicate the fraction of cells from each group that were qualitatively similar to the traces shown. Right panels: representative images of Tuj1 staining after recordings from each condition. Scale bars: 20 μm (**f**) and 100 μm (**b**, **i**).

smaller subsets of the BAM pool to determine their functionality. In many *Ascl1*-induced cells, current injection elicited action potentials, but their properties appeared to be immature, consistent with their simple neurite morphology (Fig. 5i and Supplementary Fig. 2b). MEFs infected with *Ascl1* and *Brn2* or *Myt1l* generated more mature action potentials and displayed more complex neuronal morphologies. In contrast, the majority of BAM iN cells exhibited repetitive action potentials with more mature characteristics, and displayed the most

complex neuronal morphologies. Thus, it seems likely that *Ascl1* alone is sufficient to induce some neuronal traits, such as expression of functional voltage-dependent channel proteins that are necessary for the generation of action potentials; however, co-infection of additional factors is necessary to facilitate neuronal conversion and maturation.

Discussion

Here we show that expression of three transcription factors can rapidly and efficiently convert mouse fibroblasts into functional neurons (iN cells). Although the single factor *Ascl1* was sufficient to induce immature neuronal features, the additional expression of *Brn2* and *Myt1l* generated mature iN cells with efficiencies of up to 19.5% (Supplementary Fig. 6b). Three-factor iN cells displayed functional neuronal properties such as the generation of trains of action potentials and synapse formation. These transcription factors were identified from a total of 19 candidates that we selected because of their specific expression in neural cell types or their roles in reprogramming to pluripotency (see Methods).

Despite the heterogeneity of embryonic and TTF cultures, the highly efficient nature of this process effectively rules out the possibility that directed differentiation of rare stem or precursor cells with neurogenic potential can explain our observations. Future studies will have to be performed to unequivocally demonstrate that terminally differentiated cells such as mature B or T lymphocytes can be directly converted into neurons using this approach[31,32].

It will now be of great interest to decipher the molecular mechanism of this fibroblast to neuron conversion. We assume that high expression levels of strong neural cell-fate-determining transcription factors can activate salient features of the neuronal transcriptional program. Auto-regulatory feedback and feed forward activation of downstream transcriptional regulators could then reinforce the expression of important cell-fate-determining genes and help to further stabilize the induced transcriptional program. Robust changes in transcriptional activity could also lead to genome-wide adjustments of repressive and active epigenetic features such as DNA methylation, histone modifications and changes of chromatin remodelling complexes that further stabilize the new transcriptional network[12,33]. It is possible that certain subpopulations of cells are 'primed' to respond to these factors, depending on their pre-existing transcriptional or epigenetic states[34].

The majority of iN cells described in this report are excitatory and express markers of cortical identity. A low proportion of iN cells expressed markers of GABAergic neurons, but no other neurotransmitter phenotypes were detected. Our data indicate the intriguing possibility that additional combinations of neural transcription factors might also be able to generate functional neurons whose phenotypes remain to be explored. One of the next important steps will be to generate iN cells of other specific neuronal subtypes and from human cells.

Future studies will be necessary to determine whether iN cells could represent an alternative method to generate patient-specific neurons. The generation of iN cells is fast, efficient and devoid of tumorigenic pluripotent stem cells, a key complication of induced pluripotent stem cell approaches in regenerative medicine. Therefore, iN cells could provide a novel and powerful system for studying cellular identity and plasticity, neurological disease modelling, drug discovery and regenerative medicine.

METHODS SUMMARY

Fibroblast isolation, cell culture and molecular cloning. Homozygous TauEGFP knock-in mice[21] were purchased from the Jackson Laboratories and bred with C57BL/6 mice (Taconic) to generate TauEGFP heterozygous embryos. MEFs were isolated from E14.5 embryos using a dissection microscope (Leica). Tail tips were sliced into small pieces, trypsinized and plated to derive fibroblast cultures. All fibroblasts were expanded for three passages before being used for experiments. Complementary DNAs for candidate genes were cloned into doxycycline-inducible lentiviral vectors, as described previously[35]. MEFs were infected overnight and cultured in MEF media with doxycycline for 48 h before being transferred into N3 media with doxycycline.

FACS analysis, cortical cultures, glia cultures. For glia and cortical co-cultures cells were trypsinized 8 days after infection and EGFP-positive cells were isolated using a FACS Aria II (Becton Dickinson). EGFP-positive cells were replated on 7 days *in vitro* cortical cultures from wild-type p0 mice, or alternatively, passage three primary astrocytes isolated from p5 pups (as described previously[30,36,37]).

Electrophysiology and immunofluorescence analysis. Cells were analysed at indicated times after infection. Action potentials were recorded with current-clamp whole-cell configuration. The pipette solution for current-clamp experiments contained (in mM) 123 K-gluconate, 10 KCl, 1 $MgCl_2$, 10 HEPES, 1 EGTA, 0.1 $CaCl_2$, 1 K_2ATP, 0.2 Na_4GTP and 4 glucose, pH adjusted to 7.2 with KOH. Membrane potentials were kept around −65 to −70 mV, and step currents were injected to elicit action potentials. Whole-cell currents including sodium currents, potassium currents were recorded at a holding potential of −70 mV, voltage steps ranging from −80 mV to +90 mV were delivered at 10 mV increments. Synaptic responses were measured as described previously[36,37]. For immunofluorescence experiments, cells were fixed in 4% paraformaldehyde in PBS for 10 min. Antibodies were diluted to indicated concentrations (see Methods).

Full Methods and any associated references are available in the online version of the paper at www.nature.com/nature.

Received 9 October 2009; accepted 6 January 2010.
Published online 27 January 2010.

1. Jenuwein, T. & Allis, C. D. Translating the histone code. *Science* **293**, 1074–1080 (2001).
2. Bernstein, B. E., Meissner, A. & Lander, E. S. The mammalian epigenome. *Cell* **128**, 669–681 (2007).
3. Takahashi, K. & Yamanaka, S. Induction of pluripotent stem cells from mouse embryonic and adult fibroblast cultures by defined factors. *Cell* **126**, 663–676 (2006).
4. Briggs, R. & King, T. J. Transplantation of living nuclei from blastula cells into enucleated frogs' eggs. *Proc. Natl Acad. Sci. USA* **38**, 455–463 (1952).
5. Gurdon, J. B., Elsdale, T. R. & Fischberg, M. Sexually mature individuals of *Xenopus laevis* from the transplantation of single somatic nuclei. *Nature* **182**, 64–65 (1958).
6. Campbell, K. H., McWhir, J., Ritchie, W. A. & Wilmut, I. Sheep cloned by nuclear transfer from a cultured cell line. *Nature* **380**, 64–66 (1996).
7. Tada, M., Takahama, Y., Abe, K., Nakatsuji, N. & Tada, T. Nuclear reprogramming of somatic cells by *in vitro* hybridization with ES cells. *Curr. Biol.* **11**, 1553–1558 (2001).
8. Do, J. T. & Scholer, H. R. Nuclei of embryonic stem cells reprogram somatic cells. *Stem Cells* **22**, 941–949 (2004).
9. Cowan, C. A., Atienza, J., Melton, D. A. & Eggan, K. Nuclear reprogramming of somatic cells after fusion with human embryonic stem cells. *Science* **309**, 1369–1373 (2005).
10. Silva, J. & Smith, A. Capturing pluripotency. *Cell* **132**, 532–536 (2008).
11. Blau, H. M. How fixed is the differentiated state? Lessons from heterokaryons. *Trends Genet.* **5**, 268–272 (1989).
12. Zhou, Q. & Melton, D. A. Extreme makeover: converting one cell into another. *Cell Stem Cell* **3**, 382–388 (2008).
13. Davis, R. L., Weintraub, H. & Lassar, A. B. Expression of a single transfected cDNA converts fibroblasts to myoblasts. *Cell* **51**, 987–1000 (1987).
14. Schäfer, B. W., Blakely, B. T., Darlington, G. J. & Blau, H. M. Effect of cell history on response to helix-loop-helix family of myogenic regulators. *Nature* **344**, 454–458 (1990).
15. Kondo, M. *et al.* Cell-fate conversion of lymphoid-committed progenitors by instructive actions of cytokines. *Nature* **407**, 383–386 (2000).
16. Bussmann, L. H. *et al.* A robust and highly efficient immune cell reprogramming system. *Cell Stem Cell* **5**, 554–566 (2009).
17. Feng, R. *et al.* PU.1 and C/EBPα/β convert fibroblasts into macrophage-like cells. *Proc. Natl Acad. Sci. USA* **105**, 6057–6062 (2008).
18. Xie, H., Ye, M., Feng, R. & Graf, T. Stepwise reprogramming of B cells into macrophages. *Cell* **117**, 663–676 (2004).
19. Cobaleda, C., Jochum, W. & Busslinger, M. Conversion of mature B cells into T cells by dedifferentiation to uncommitted progenitors. *Nature* **449**, 473–477 (2007).
20. Zhou, Q., Brown, J., Kanarek, A., Rajagopal, J. & Melton, D. A. *In vivo* reprogramming of adult pancreatic exocrine cells to β-cells. *Nature* **455**, 627–632 (2008).
21. Tucker, K. L., Meyer, M. & Barde, Y. A. Neurotrophins are required for nerve growth during development. *Nature Neurosci.* **4**, 29–37 (2001).
22. Wernig, M. *et al.* Tau EGFP embryonic stem cells: an efficient tool for neuronal lineage selection and transplantation. *J. Neurosci. Res.* **69**, 918–924 (2002).
23. Lee, J. E. *et al.* Conversion of *Xenopus* ectoderm into neurons by NeuroD, a basic helix-loop-helix protein. *Science* **268**, 836–844 (1995).
24. Guillemot, F. *et al.* Mammalian achaete-scute homolog 1 is required for the early development of olfactory and autonomic neurons. *Cell* **75**, 463–476 (1993).
25. Farah, M. H. *et al.* Generation of neurons by transient expression of neural bHLH proteins in mammalian cells. *Development* **127**, 693–702 (2000).
26. Guillemot, F. Cellular and molecular control of neurogenesis in the mammalian telencephalon. *Curr. Opin. Cell Biol.* **17**, 639–647 (2005).
27. Escurat, M., Djabali, K., Gumpel, M., Gros, F. & Portier, M. M. Differential expression of two neuronal intermediate-filament proteins, peripherin and the

low-molecular-mass neurofilament protein (NF-L), during the development of the rat. *J. Neurosci.* **10,** 764–784 (1990).
28. Beard, C., Hochedlinger, K., Plath, K., Wutz, A. & Jaenisch, R. Efficient method to generate single-copy transgenic mice by site-specific integration in embryonic stem cells. *Genesis* **44,** 23–28 (2006).
29. Christopherson, K. S. *et al.* Thrombospondins are astrocyte-secreted proteins that promote CNS synaptogenesis. *Cell* **120,** 421–433 (2005).
30. Wu, H. *et al.* Integrative genomic and functional analyses reveal neuronal subtype differentiation bias in human embryonic stem cell lines. *Proc. Natl Acad. Sci. USA* **104,** 13821–13826 (2007).
31. Hochedlinger, K. & Jaenisch, R. Monoclonal mice generated by nuclear transfer from mature B and T donor cells. *Nature* **415,** 1035–1038 (2002).
32. Hanna, J. *et al.* Direct reprogramming of terminally differentiated mature B lymphocytes to pluripotency. *Cell* **133,** 250–264 (2008).
33. Jaenisch, R. & Young, R. Stem cells, the molecular circuitry of pluripotency and nuclear reprogramming. *Cell* **132,** 567–582 (2008).
34. Yamanaka, S. Elite and stochastic models for induced pluripotent stem cell generation. *Nature* **460,** 49–52 (2009).
35. Wernig, M. *et al.* A drug-inducible transgenic system for direct reprogramming of multiple somatic cell types. *Nature Biotechnol.* **26,** 916–924 (2008).
36. Maximov, A., Pang, Z. P., Tervo, D. G. & Sudhof, T. C. Monitoring synaptic transmission in primary neuronal cultures using local extracellular stimulation. *J. Neurosci. Methods* **161,** 75–87 (2007).
37. Maximov, A. & Sudhof, T. C. Autonomous function of synaptotagmin 1 in triggering synchronous release independent of asynchronous release. *Neuron* **48,** 547–554 (2005).

Supplementary Information is linked to the online version of the paper at www.nature.com/nature.

Acknowledgements We would like to thank S. Marro and P. Lovelace for help with FACS sorting, S. Hafeez and Y. Huh for assistance with molecular cloning and mouse husbandry, and K. Jann for assistance with the diagram in Fig. 1. We would also like to thank I. Graef, R. Bajpai, J. Wysocka, J.-R. Lin and J.-Y. Chen for contributing reagents and help with analysis. This work was supported by start-up funds from the Institute for Stem Cell Biology and Regenerative Medicine at Stanford (M.W.), the Donald E. and Delia B. Baxter Foundation (M.W.), an award from William Stinehart Jr and the Reed Foundation (M.W.), the National Institute of Health Training Grant 1018438-142-PABCA (A.O.) and the Ruth and Robert Halperin Stanford Graduate Fellowship (T.V.). Z.P.P. is supported by NARSAD Young Investigator Award and NIH/NINDS Epilepsy Training Grant 5T32NS007280.

Author Contributions T.V., A.O. and M.W. designed and conceived the experiments. T.V., Y.K. and M.W. produced the lentiviral vectors. T.V. and A.O. performed the lentiviral infections, isolated the fibroblasts and completed the molecular characterization of the iN cells. Z.P.P. and T.C.S. designed, performed and analysed the electrophysiological assays. T.V., A.O., Z.P.P., T.C.S. and M.W. wrote and edited the manuscript and produced the figures.

Author Information Reprints and permissions information is available at www.nature.com/reprints. The authors declare no competing financial interests. Correspondence and requests for materials should be addressed to M.W. (wernig@stanford.edu).

METHODS

Embryonic fibroblast isolation. Homozygous TauEGFP knock-in mice[21] were purchased from the Jackson Laboratories and bred with C57BL/6 mice (Taconic) to generate TauEGFP heterozygous embryos. BALB/c mice were purchased from Taconic. Rosa26-rtTA mice were obtained from R. Jaenisch[28]. MEFs were isolated from E14.5 embryos under a dissection microscope (Leica). The head, vertebral column (containing the spinal cord), dorsal root ganglia and all internal organs were removed and discarded to ensure the removal of all cells with neurogenic potential from the cultures. The remaining tissue was manually dissociated and incubated in 0.25% trypsin (Sigma) for 10–15 min to create a single cell suspension. The cells from each embryo were plated onto a 15-cm tissue culture dish in MEF media (Dulbecco's Modified Eagle Medium; Invitrogen) containing 10% fetal bovine serum (FBS; Hyclone), β-mercaptoethanol (Sigma-Aldrich), non-essential amino acids, sodium pyruvate and penicillin/streptomycin (all from Invitrogen). Cells were grown at 37 °C for 4–7 days until confluent, and then split once before being frozen. After thawing, cells were cultured on 15-cm plates and allowed to become confluent before being split onto plates for infections using 0.25% trypsin. Postnatal TTFs were prepared by removing the bottom third of tail from 3-day-old pups using surgical scissors. Cells were rinsed in ethanol, washed with HBSS (Sigma), and then dissociated using scissors and 0.25% trypsin. TTFs were cultured in MEF media until confluent and passaged once before being pooled together and frozen down for further use.

Cell culture, molecular cloning and viral infections. We had three criteria for identifying candidates with neuron-inducing activity: (1) we reasoned that cell-fate-inducing factors should be enriched in the gene category of transcriptional regulators. (2) We included factors previously involved in reprogramming to pluripotency (*Klf4*, c-*Myc* and *Sox2*). (3) We searched for genes specifically expressed in neural tissues. Those were selected based on published expression arrays of MEFs, embryonic stem cells and neural progenitor cells retrieved from the Gene Expression Omnibus database (GSE8024, http://www.ncbi.nlm.nih.gov/gds) and the EST Profile function of NCBI's Unigene database (http://www.ncbi.nlm.nih.gov/unigene). cDNAs for the factors included in the 19 factor pool were cloned into lentiviral constructs under the control of the tetracycline operator[35]. Replication-incompetent, VSVg-coated lentiviral particles were packaged in 293T cells as described[35]. Passage three TauEGFP and BALB/c MEFs were infected in MEF media containing polybrene (8 μg ml^{-1}). After 16–20 h in media containing lentivirus, the cells were switched into fresh MEF media containing doxycycline (2 μg ml^{-1}) to activate expression of the transduced genes. After 48 h in MEF media with doxycycline (Sigma), the media was replaced with N3 media[22] containing doxycycline. The media was changed every 2–3 days for the duration of the culture period. For BrdU experiments, 10 μM BrdU was added to the culture media and was maintained throughout media changes until the cells were fixed.

Immunofluorescence, RT–PCR and flow cytometry. Neuronal cells were defined as cells that stained positive for Tuj1and had a process at least three times longer than the cell body. For immunofluorescence staining, cells were washed with PBS and then fixed with 4% paraformaldehyde for 10 min at room temperature. Cells were then incubated in 0.2% Triton X-100 (Sigma) in PBS for 5 min at room temperature. After washing twice with PBS, cells were blocked in a solution of PBS containing 4% BSA, 1% FBS for 30 min at room temperature. Primary and secondary antibodies were diluted in a solution of PBS containing 4% BSA and 1% FBS. Fields of cells for staining were outlined with a PAP pen (DAKO). Primary and secondary antibodies were typically applied for 1 h and 30 min, respectively. Cells were washed three times with PBS between primary and secondary staining. For anti-BrdU staining, cells were treated with 2 N HCl in PBS for 10 min and washed twice with PBS before permeabilization with Triton X-100 (Sigma). The following antibodies were used for our analysis: goat anti-choline acetyltransferase (Millipore, 1:100), rabbit anti-GABA (Sigma, 1:4,000), rabbit-GFAP (DAKO, 1:4,000), mouse anti-MAP2 (Sigma, 1:500), mouse anti-NeuN (Millipore, 1:100), mouse anti-peripherin (Sigma, 1:100), mouse anti-Sox2 (R&D Systems, 1:50), rabbit anti-serotonin (Biogenesis, 1:1,000), rabbit anti-Tuj1 (Covance, 1:1,000), mouse anti-Tuj1 (Covance, 1:1,000), goat anti-Brn2 (Santa Cruz Biotechnology, 1:100), mouse anti-BrdU (Becton Dickinson, 1:3.5), mouse anti-calretinin (DAKO, 1:100), sheep anti-tyrosine hydroxylase (Pel-Freez, 1:1,000), E028 rabbit anti-synapsin (gift from T. Südhof, 1:500), guinea-pig anti-vGLUT1 (Millipore, 1:2,000), mouse anti-GAD6 (Developmental Studies Hybridoma Bank (DSHB), 1:500), mouse anti-Pax3 (DSHB, 1:250), mouse anti-Pax6 (DSHB, 1:50), mouse anti-Pax7 (DSHB, 1:250), mouse anti-Nkx2.2 (DSHB, 1:100), mouse anti-Olig1 (NeuroMab, 1:100). FITC- and Cy3-conjugated secondary antibodies were obtained from Jackson Immunoresearch. Alexa-488-, Alexa-546- and Alexa-633-conjugated secondary antibodies were obtained from Invitrogen. TauEGFP-expressing cells were analysed and sorted on a FACS Aria II (Becton Dickinson). Flow cytometry data were analysed using Flowjo (Tree Star). After sorting, cells were plated on cortical cultures or glia cultures derived from neonatal brains. Cells were kept in 50% N3 media and 50% growth media (see media composition below) and 2 μg ml^{-1} doxycycline for 1 week before being switched to growth media without doxycycline until electrophysiological analysis was completed. For RT–PCR analysis, RNA was isolated using Trizol (Invitrogen) following the manufacturer's instructions, treated with DNase (NEB) and 1.5 μg was reverse-transcribed with Superscript II (Invitrogen). PCR was performed using the following primers: *Sox1*, forward 5′-TCGAGCCCTTCTCACTTGTT-3′, reverse 5′-TTGATGCATTTTGGGGGTAT-3′; *Sox10*, forward 5′-GAACTGGGCAAGG TCAAGAA-3′, reverse 5′-CGCTTGTCACTTTCGTTCAG-3′; β-actin, forward 5′-CGTGGGCCGCCCTAGGCACCA-3′, reverse 5′-CTTAGGGTTCAGGGGG GC-3′. PCR products were analysed on a 1% gel.

Efficiency calculation. The following method was used to calculate the efficiency of neuronal induction. The total number of Tuj1^{+} cells with a neuronal morphology, defined as cells having a circular, three-dimensional appearance that extend a thin process at least three times longer than their cell body, were quantified 12 days after infection. This estimate was based on the average number of iN cells present in 30 randomly selected ×20 visual fields. The area of a ×20 visual field was then measured, and we used this estimated density of iN cells to determine the total number of neurons present in the entire dish. We then divided this number by the number of cells plated before infection to get a percentage of the starting population of cells that adopted neuron-like characteristics.

Cortical cultures. Primary cortical neurons were isolated from newborn wild-type mice as described[36] with modifications. Briefly, cortices were dissociated by papain (10 U ml^{-1}, with 1 μM Ca^{2+}, and 0.5 μM EGTA) digestions and plated on Matrigel-coated circle glass coverslips (∅ 11 mm). The neurons were cultured *in vitro* in growth media consisting of MEM (Invitrogen) supplemented with B27 (Invitrogen), glucose, transferrin, FBS and Ara-C (Sigma).

Glia cell isolation. Forebrains were dissected from postnatal day five wild-type mice and were manually dissociated into ~0.5 mm^2 pieces in a total of 2 ml of HBSS. A total of 500 μl of 2.5% trypsin and 1% DNase were added and dissociated tissue was incubated at 37 °C for 15 min. Solution was mixed every 5 min. The supernatant was then transferred into 1.5 ml FBS. A total of 4 ml HBSS, 500 μl 2.5% trypsin, and 500 μl DNase were again added to the remaining dissociated tissue and incubated at 37 °C for 15 min, mixing every 5 min. The supernatant was again removed and added to the FBS-containing solution. Using a pipette, the remaining tissue was further dissociated and passed through a 70 μM nylon mesh filter (BD Biosciences) into the FBS-containing solution. The cell mixture was then spun at 1,000 r.p.m. for 5 min and re-suspended in MEF media. Glia cells were passaged three times before culturing with MEF or TTF-derived iN cells. Contaminating neurons in p3 glia cell cultures could not be detected when stained for either Tuj1 or MAP2.

Electrophysiology. Recordings were performed from MEF- and tail-cell-derived iN cells at 8, 12 and 20 days after viral infection, or 7–13 days after co-culturing with cortical neurons. Spontaneous or evoked synaptic responses were recorded in the whole-cell voltage-clamp mode. Evoked synaptic responses were triggered by 1-ms current injection through a local extracellular electrode (FHC concentric bipolar electrode, Catalogue number CBAEC75) with a Model 2100 Isolated Pulse Stimulator (A-M Systems), and recorded in whole-cell mode using a Multiclamp 700B amplifier (Molecular Devices)[37]. Data were digitized at 10 kHz with a 2 kHz low-pass filter. The whole-cell pipette solution for synaptic current recordings contained (in mM): CsCl 135, HEPES 10, EGTA 1, Mg-ATP 4, Na_4GTP 0.4, and QX-314 10, pH 7.4. The bath solution contained (in mM): NaCl 140, KCl 5, $CaCl_2$ 2, $MgCl_2$ 2, HEPES 10, and glucose 10, pH 7.4. IPSCs were pharmacologically isolated by addition of 50 μM D-AP5 and 20 μM CNQX to the bath solution. EPSCs were pharmacologically isolated by addition of 30 μM picrotoxin. Data were analysed using Clampfit 10.02 (Axon Instruments). Action potentials were recorded with the current-clamp whole-cell configuration. The pipette solution for current-clamp experiments contained (in mM): 123 K-gluconate, 10 KCl, 1 $MgCl_2$, 10 HEPES, 1 EGTA, 0.1 $CaCl_2$, 1 K_2ATP, 0.2 Na_4GTP, and 4 glucose, pH adjusted to 7.2 with KOH. Membrane potentials were kept around −65 to −70 mV, and step currents were injected to elicit action potential. Whole-cell currents including sodium currents and potassium currents were recorded at a holding potential of −70 mV; voltage steps ranging from −80 mV to +90 mV were delivered at 10-mV increments.